Journal of the Geological Society, *London*, Vol. **166**, 2009, pp. 1123–1133. doi: 10.1144/0016-76492009-070.

Late Jurassic palaeoclimatic change from clay mineralogy and gamma-ray spectrometry of the Kimmeridge Clay, Dorset, UK

STEPHEN P. HESSELBO[1]*, JEAN-FRANÇOIS DECONINCK[2], JENNIFER M. HUGGETT[3] & HELEN S. MORGANS-BELL[1]

[1]*Department of Earth Sciences, University of Oxford, Parks Road, Oxford OX1 3PR, UK*

[2]*Université de Bourgogne, UMR CNRS 5561 Biogéosciences, 6 Boulevard Gabriel, 21000 Dijon, France*

[3]*Department of Mineralogy, The Natural History Museum, Cromwell Road, London SW7 5BD, UK*

**Corresponding author (e-mail: stephen.hesselbo@earth.ox.ac.uk)*

Abstract: The Late Jurassic was a time of increasing aridity in NW Europe. Here, a new clay mineral dataset is presented from a 600 m thick composite core through the Kimmeridge Clay Formation, southern England. Clay mineral assemblages comprise mainly illite and kaolinite, with minor randomly interstratified illite–smectite mixed-layer clays. SEM observations indicate that clay minerals are mainly detrital, except in silty strata of late Tithonian age, which contain abundant pore-filling kaolinite aggregates. Th/K ratios determined from gamma-ray spectrometry mirror palaeoclimatically significant variations in kaolinite/illite ratios, with notable exception where diagenetic kaolinite occurs. Comparison with age-equivalent strata identifies regional cyclic variations in clay minerals at the 100–300 m scale. Small-scale (10–20 m) variations in clay minerals and Th/K also occur. It is proposed that the region experienced progressively intense humidity through the Kimmeridgian, followed by a return to more arid conditions during the early Tithonian. Following a mid-Tithonian peak in aridity (the 'Hudlestoni Event'), more humid climatic conditions returned prior to the development of latest Tithonian intense aridity. Late Jurassic climate was apparently subject to synchronously cyclic changes across a broad area of the Laurasian continent. Such changes could not have resulted from mountain building or continental rotations.

Supplementary material: Clay data are available at http://www.geolsoc.org.uk/SUP18376.

The aim of the present study is to use clay mineral and spectral gamma-ray data to refine the proxy record of palaeoclimate change through the Late Jurassic in southern England. A long-term evolution from relatively humid to relatively arid conditions through this succession has been long established based on consideration of a variety of sedimentological and palaeontological data (Hallam 1984). More focused analyses have highlighted what appears to be a sudden change from humid to semi-arid climates in the mid-Tithonian (*hudlestoni* Ammonite Biozone) based on observations from the Upper Kimmeridge Clay outcrop in southern England, in particular using evidence from clay mineralogy, palaeoecology, early carbonate diagenesis, and sedimentary facies (Wignall & Ruffell 1990).

Inferences from clay mineralogy from the UK and France, especially the ratios between the clay minerals kaolinite and illite, have been summarized and discussed by Hallam *et al*. (1991) and Deconinck (1993); these workers documented the near disappearance of kaolinite around the Jurassic–Cretaceous boundary. As reviewed by Thiry (2000), the ratio between kaolinite and illite is deemed climatically significant because the formation of kaolinite in soils is favoured under hot humid conditions, and although the mechanisms by which the climate signal is encoded in the sedimentary record is complex, the clay mineral assemblages of marine deposits may be expected to yield a climate signal that is time-averaged and from a broad region. In the case of the Late Jurassic of NW Europe the inference of palaeoclimatic significance is borne out by consistency with other evidence such as palynological data or the occurrence of unambiguously climatically sensitive sedimentary deposits such as evaporites (e.g. Hallam *et al*. 1991).

Consideration of regional clay mineral distributions, together with limited palaeobotanical data, has also been used to argue that aridification took place diachronously during the Late Jurassic in the present NW European area, occurring later in the more northerly locations (Hallam 1993; Wignall & Pickering 1993). It has also been hypothesized that the regional aridification was a response to Cimmeride mountain building and a rain-shadow effect affecting easterly air flows (Hallam 1984, 1993). In addition, quantitative sporomorph data (i.e. changing dominance of climate-sensitive taxa within lowland and coastal ecological groups) have been used to construct a palaeoclimate curve for the North Sea region (Abbink *et al*. 2001). At a coarse stratigraphic resolution, a stepwise warming and aridification is inferred through the Late Jurassic, and the 'aridification event' identified by Wignall & Ruffell (1990) in the Tithonian (*hudlestoni* Zone) has been hypothetically linked to arrival of cool high-latitude waters by means of an opening Boreal Ocean–Tethys Ocean link (Abbink *et al*. 2001). On a larger scale still, the changes in terrestrial biomes and climate-sensitive sedimentary facies across the whole Laurasian landmass have led some workers (Rees *et al*. 2000; Ziegler *et al*. 2003) to propose that the Late Jurassic increase in aridity was actually an expression of clockwise rotation of Laurasia.

In the context of this previous work, we seek here to document a much more detailed history of palaeoclimate change based on a relatively continuous marine record that is well calibrated in terms of age assignment (e.g. Weedon *et al*. 1999, 2004;

Gradstein *et al*. 2004) and sedimentological setting. A specific question addressed is whether the inferred aridification took place locally as a single event, or whether, in contrast, the change was part of a longer-term pattern of cyclic variation occurring over a wide area.

The new data come from boreholes drilled in 1997 at two sites close to the Kimmeridge Clay Formation type-section in southern England (Fig. 1; Gallois 2000; Morgans-Bell *et al*. 2001). The boreholes, at Swanworth Quarry and Metherhills, were drilled as part of a joint Natural Environment Research Council and industry-sponsored project, Rapid Global Geological Events (RGGE). Unlike the adjacent coastal exposure, the boreholes sample the entire Kimmeridge Clay (representing most of the Kimmeridgian and Tithonian Stages) and, uniquely, permit a comparison between core-derived analytical data and downhole geophysical logs. Some previously unpublished data generated from the RGGE project (Chambers 2006) have been presented and discussed briefly by Jeans (2006).

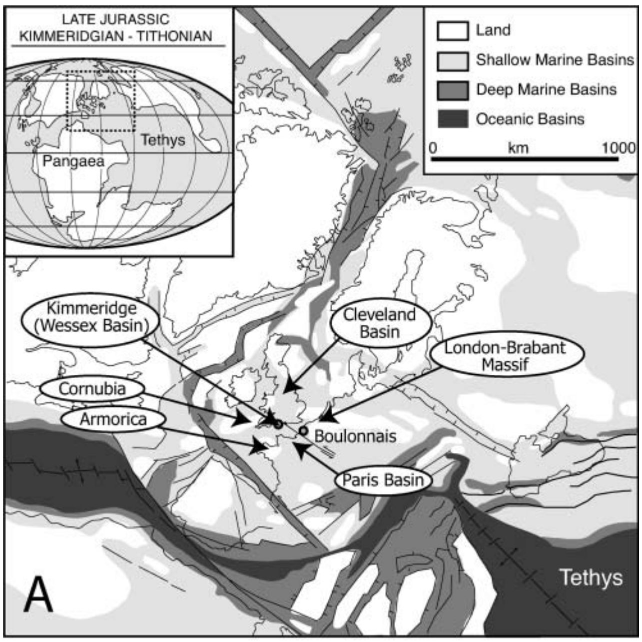

Series	Stage	Wessex Basin
Early Cretaceous	Berriasian	Purbeck Group
Late Jurassic	Tithonian	Portland Group
	Tithonian / Kimmeridgian	Kimmeridge Clay
	Oxfordian	Corallian Group

B

Fig. 1. (**a**) Palaeogeographic setting and locations referred to in text (modified from Ziegler 1990). (**b**) Summary lithostratigraphy and chronostratigraphy for the Wessex Basin (Cope *et al*. 1980; Ogg *et al*. 1994).

In addition to standard X-ray diffraction (XRD) determination of clay mineral assemblages, we supplement the analytical data by consideration of downhole spectral gamma-ray logs. A relationship between spectral gamma-ray characteristics of rocks and their clay mineralogy has been postulated for some time (Hassan & Hossin 1975; Serra *et al*. 1980; Quirein *et al*. 1982). However, there are surprisingly few studies that calibrate spectral gamma-ray data with semi-quantitative XRD determinations of clay mineralogy through an extended stratigraphic sequence (Hesselbo 1996; Ruffell & Worden 2000; Ruffell *et al*. 2002; Deconinck *et al*. 2003; Schnyder *et al*. 2006). These studies have all demonstrated a relationship between Th/K ratio determined by gamma-ray spectrometry and primary clay mineralogy, particularly a positive correlation between Th/K ratio and kaolinite/illite ratio.

Clay mineral analysis

About 200 samples were taken from the cores at *c*. 2.5 m spacing through *c*. 550 m of section. Somewhat higher resolution sampling (*c*. 1–2 m) was carried out for three sub-intervals where definition of small-scale cyclic variation required higher sample density: 460–430 m, 240–210 m and 145–115 m depth. Clay mineral associations were studied using XRD of oriented mounts. Each crushed sample was decarbonated using 0.2N hydrochloric acid. Excess acid was removed by successive washing with deionized water (Holtzapffel 1985). The clay fraction (<2 μm) was separated by sedimentation and centrifugation. (The <2 μm fraction should exclude most diagenetic kaolinite because this has a typical particle size of 5–10 μm when it has replaced feldspar and an order of magnitude greater when it pseudomorphs mica.) X-ray diagrams were obtained using a Philips PW diffractometer with CuK_{α} radiation and a Ni filter. For each sample, three X-ray analyses were performed: after air-drying, ethylene-glycol solvation, and heating at 490 °C for 2 h. The identification of clay minerals was made according to the position of the (001) series of basal reflections on the three X-ray diagrams (Brown & Brindley 1980; Moore & Reynolds 1997). Relative proportions of clay minerals are based on the peak heights and areas summed to 100%, the relative error being typically *c*. 10%. The relative abundance of two clay species is estimated using the ratio between the intensity of the basal reflection of each mineral. The relative abundance of illite and kaolinite can be approximated from the ratio between the intensity of the diffraction peak at 7 Å (basal reflection (001) of kaolinite), and that at 10 Å (basal reflection (001) of illite). The diffraction peak at 7 Å comprises the basal reflection of kaolinite and the (002) reflection of chlorite. Chlorite occurs only as a minor component of the clay fraction in most of the rocks studied, except in samples from 570 to 470 m, and sporadically from 470 to 390 m depth; the kaolinite–chlorite reflection doublet at 3.5 Å is easily split and can be used to assess the relative proportions.

The clay mineral assemblages are dominated by illite and kaolinite, with subsidiary quantities of random illite–smectite (I–S) mixed layers. Mixed-layer I–S expanding to 17 Å after glycolation occurs sporadically between 470 and 430 m, and in a sample at *c*. 42 m. Chlorite occurs consistently in samples from 570 to 470 m, and sporadically from 470 to 390 m depth. Quartz occurs throughout in small quantities in the clay fraction. This overall composition, previously mentioned by Jeans (2006), is expressed by some typical XRD patterns shown in Figure 2.

There are clear large-scale trends in the ratio of kaolinite to illite and these are shown in Figure 3. In the condensed basal

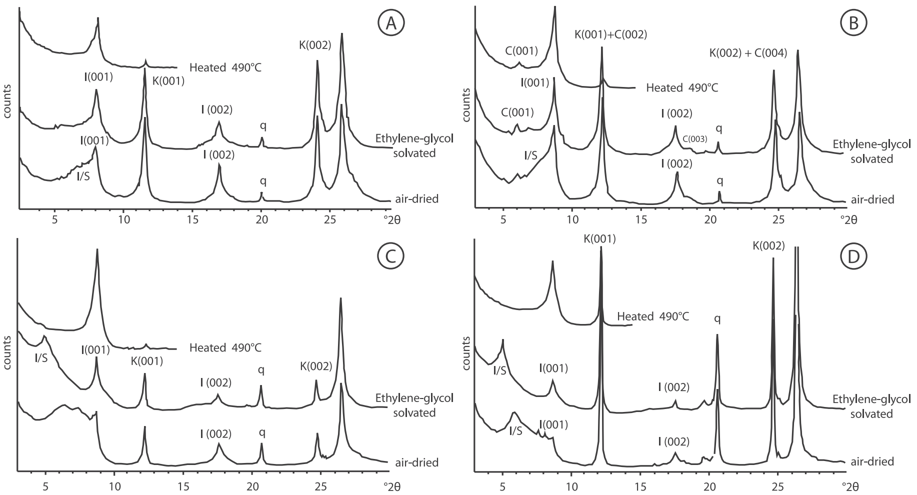

Fig. 2. Typical X-ray diagrams of Kimmeridge Clay samples. (**a**) Mixture of illite (I), illite–smectite mixed layers (I–S), and kaolinite (K) with small quantities of quartz (q) (Sample MH1/12/2; 398.4 m). (**b**) X-ray diagram showing the additional occurrence of chlorite (C) (Sample MH1/23/8; 428.74 m). (**c**) X-ray diagram showing the occurrence of I–S expanding to 17 Å after ethylene-glycol solvation. This type of XRD is uncommon in the Kimmeridge Clay Formation (Sample SQ1/23/2; 51.74 m). (**d**) X-ray diagram showing the sharpness of the kaolinite peaks, suggesting an authigenic contribution of this mineral (Sample SQ1/22/2; 49.17 m).

baylei Zone of the Kimmeridge Clay Formation (Early Kimmeridgian), kaolinite/illite ratios vary abruptly between *c*. 1 and 2.5. Above this level and through the bulk of the Kimmeridgian part of Kimmeridge Clay Formation, there is a progressive increase in kaolinite/illite ratio that peaks at about 2.5 in the *autissiodorensis* Zone. From this level upwards, through the Early Tithonian part of the Kimmeridge Clay, there is a decline in kaolinite/illite ratios to minimum values of *c*. 0.7 in the middle *hudlestoni* Zone. From this level upwards through the *pectinatus* to lower *rotunda* zones there is a modest increase in kaolinite/illite ratios to just above 1.5, and above this stratigraphic level the values decrease again to 0.8 in the lower *fittoni* Zone. Finally, at the top of the sampled formation in the *fittoni* Zone, there is a single large spike to a kaolinite/illite ratio of five. This last interval has more smectite layers in the I–S mixed layers, and particularly well-crystallized kaolinite compared with the remainder of the formation.

At approximately the 10–20 m scale, cyclic variations in kaolinite/illite ratios are also apparent, but generally showing a relatively small amplitude (<1). These cycles are well defined by multiple data points through most of the formation. An isolated high kaolinite/illite ratio of 2.80 occurs in a sample at 236 m depth, corresponding to the lower *hudlestoni* Zone, and we note also that Jeans (2006) has highlighted stratigraphically very restricted high relative kaolinite content in the White Stone Band in the *pectinatus* Zone. The amplitudes of cycles at the 10–20 m scale are largest in the middle and upper part of the formation, and there are notable, relatively thin, intervals with particularly low kaolinite/illite ratios in the *autissiodorensis*, *scitulus* and *pallasioides* zones (marked with asterisks in Fig. 3).

Changes in clay kaolinite/illite ratios in the vicinity of the *hudlestoni* Zone are of particular interest because this is the part of the section where clay mineral data have been generated previously (Wignall & Ruffell 1990). The pattern of changes in ratio that were reported is confirmed in the present study, even though the actual ratio values are different. What also becomes very clear, however, is that the low kaolinite/illite ratios in the middle *hudlestoni* Zone constitute a ‘Hudlestoni Event’, and represent the culmination of a longer-term trend that began in the *elegans* Zone (= earliest Tithonian); above the *hudlestoni* Zone the average kaolinite/illite ratio returns to a somewhat higher level through several zones before again declining upwards.

Spectral gamma ray

There have been several previous studies of the gamma-ray log signatures of the Kimmeridge Clay and most of these have focused on the total gamma-ray signature as a tool for correlation and lithological interpretation (Gallois 1973; Whittaker *et al*. 1985; Penn *et al*. 1986; Brereton *et al*. 2001; Taylor *et al*. 2001), or as a data source for cyclostratigraphy (Melnyk *et al*. 1992, 1994). An exception is the work of Myers & Wignall (1987) and Wignall & Myers (1988), who discussed the distribution of K, Th, and U determined by gamma-ray spectrometry for segments of the Kimmeridge Clay outcrop, using data collected with a hand-held detector, and comparing these with palaeontological evidence for bottom-water oxygenation and water depth. The Th and K content of a mudstone is known to be related to clay mineralogy, and where the sediment also contains significant potassium feldspar or mica, as is likely in silt-rich bands, an influence from these minerals may also be expected (see summary by Rider 1996).

The ‘sample’ interval of the gamma-ray log used in the present study is 0.15 m. Because the downhole tool detects gamma rays generated from greater than 15 cm distance through the formation, each data point will include gamma rays derived from outside the 15 cm window over which counts are made as the tool is pulled up the borehole. As a result, the gamma-ray curve is a smoothed representation of the true gamma-ray profile of the section. However, 95% of the gamma rays counted will be from <20 cm radius away from the detector (e.g. Rider 1996).

At the large scale, Th/K ratios remain relatively constant with values of *c*. 4 through the Kimmeridge Clay of Kimmeridgian age up to the *autissiodorensis* Zone, above which point ratios increase to *c*. 5 (Fig. 3). Above this level, in strata of Tithonian age, ratios decrease to a low point of <3 in the upper *hudlestoni* Zone and then return to values of *c*. 4. At the scale of 10–20 m, cyclic variation also occurs in the Th/K ratio data. This high-frequency variation occurs at high amplitude, and although some of the low-value and high-value spikes are within carbonate-cemented horizons (stone bands), this is not always the case. On the basis that carbonate-cemented horizons have small absolute Th and K values, and therefore less robust counting statistics, it may be supposed that the Th/K ratios for these horizons are less reliable than for the bulk of the formation. Therefore a filter has been applied to the data shown in Figure 3, highlighting in black

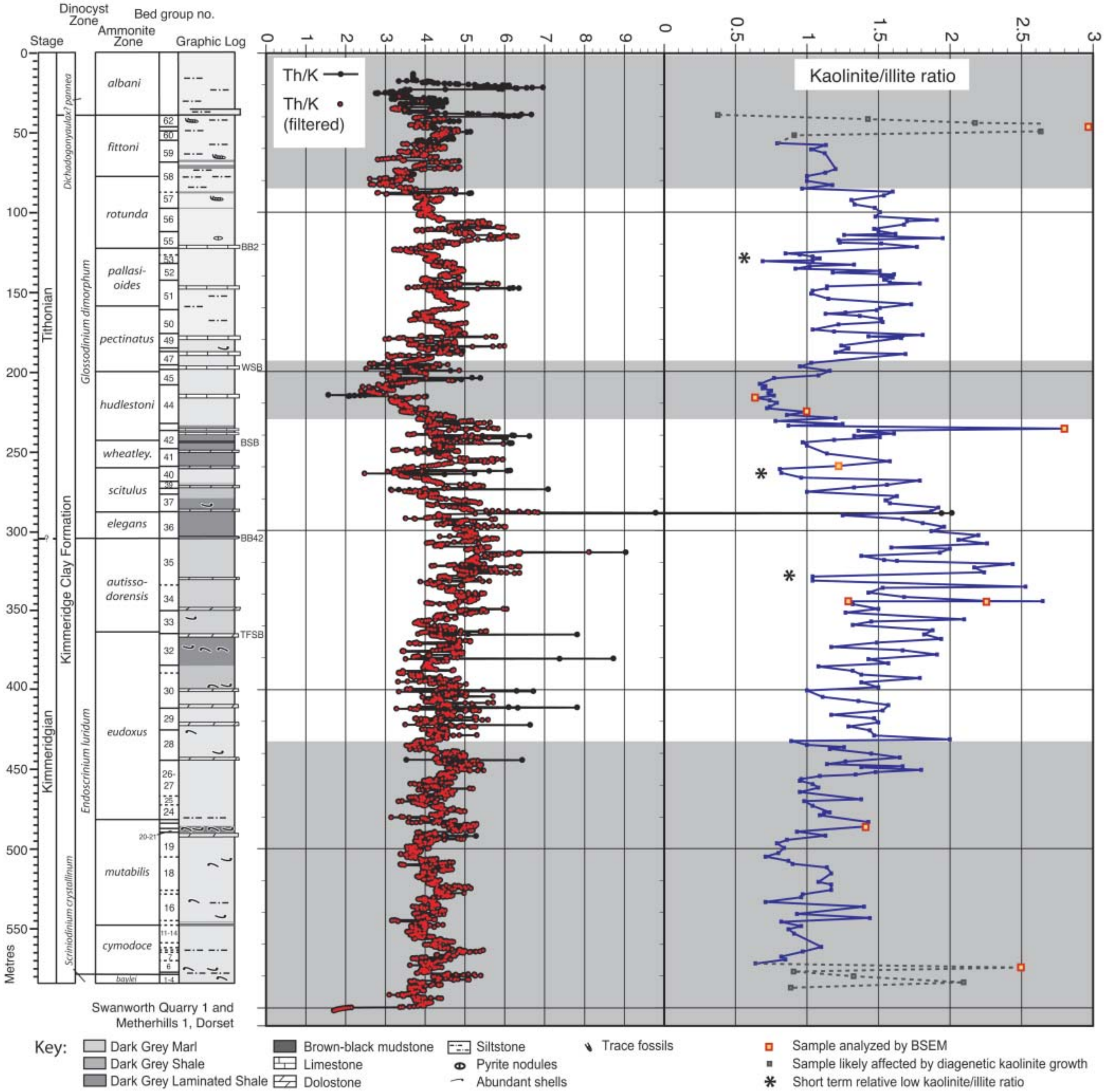

Fig. 3. Composite lithological log, Th/K ratio from downhole spectral gamma-ray log (SGR), and kaolinite/illite ratio from XRD of core samples. Graphic log and ammonite biostratigraphy for the Swanworth Quarry 1 (40–375 m) and Metherhills (375–bottom) boreholes are from Morgans-Bell *et al*. (2001). Marker beds: TFSB, The Flats Stone Band; BB42, Blake's Bed 42; BSB, Blackstone Band; WSB, White Stone Band; BB2, Blake's Bed 2. Large shaded boxes indicate zones of relatively high and relatively low primary kaolinite/illite ratios.

those data points with Th <4.5 ppm or K <1.5%. This filter results in removal of the most extreme variations but does not completely eradicate the spikes, indicating that some real variations in chemical composition are represented by these atypically high and low values.

Changes in clay mineralogy and Th/K ratios occur broadly in parallel at the scales of *c*. 100–200 m and locally *c*. 10–20 m. Correlations at the 10–20 m scale are particularly apparent from 520 to 430 m and from 330 to 75 m depth (Fig. 3). Visual inspection suggests that the correlation to be best in the middle and upper parts of the formation. A cross plot of Th/K v. kaolinite/illite ratio bears out this observation (Fig. 4). Amplitudes of the 10–20 m scale cycles are relatively small in the middle part of the formation, where there is a poor correlation with clay mineral cycles at the same scale.

Clay mineral diagenesis

In the SW region of the Wessex Basin, the Kimmeridge Clay Formation is overlain by the Portland and Purbeck groups (*c*. 110 m), and by later Cretaceous units including the Wealden Group (*c*. 600 m), the Lower Greensand, Gault and Upper

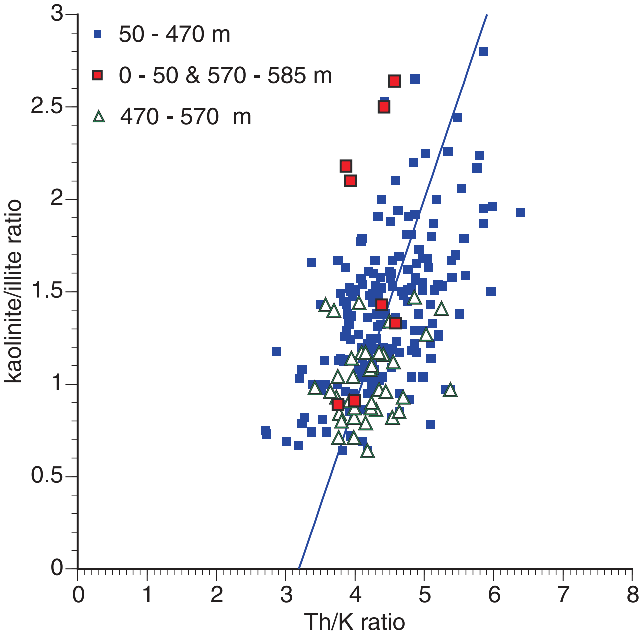

Fig. 4. Cross plot of downhole Th/K (SGR) v. kaolinite/illite (XRD) from core samples. Data points plotting well above the linear regression line ($R^2 = 0.43$) are likely to contain authigenic kaolinite.

Greensand (*c*. 300 m), and the Chalk (*c*. 500 m) (e.g. Chadwick 1985; Butler 1998). Therefore, the total burial depth of the Kimmeridge Clay Formation probably did not exceed 1500 m. Several observations suggest that the influence of diagenesis on clay minerals is minimal. (1) There is no regular evolution of clay-mineral assemblages from top to bottom of the boreholes that would be indicative of burial diagenesis. (2) The lower Purbeck Group, a somewhat younger lithostratigraphic unit of latest Jurassic and earliest Cretaceous age, has a clay fraction containing abundant smectite, (Deconinck 1987; Schnyder *et al*. 2006), which is considered the most sensitive clay mineral to diagenetic effects and is rapidly transformed into illite–smectite mixed layers with depth at burial temperatures >80 °C, provided that there is a supply of potassium for the illite. (3) Estimates of the organic maturity parameter T_{max} (corresponding to the laboratory temperature recorded for the S2 pyrolysis peak) range from 415 to 425 °C in the Kimmeridge Clay Formation of Dorset and indicate an organic maturation level below the oil-window (Scotchman 1987*a*,*b*, 1989; Lallier-Vergès *et al*. 1993). In many sedimentary successions, such values are compatible with the occurrence of smectites (e.g. Caron *et al*. 1999; Schnyder *et al*. 2006).

SEM and thin-section observations were used by Macquaker & Gawthorpe (1993) to conclude that the clay-rich mudstones of the Kimmeridge Clay of the Wessex Basin are composed predominantly of detrital clays, including muscovite (illite), illite–smectite mixed layers, and kaolinite. A somewhat different view was presented by Burley & Macquaker (1992), who documented from SEM data the occurrence of authigenic kaolinite within microfossil tests, and as a pore-filling component within silty facies of the Kimmeridge Clay, but without reference to stratigraphic distribution.

In discussion of the variation in the kaolinite/illite ratios in the White Stone Band (compare Fig. 3; not sampled in the present study), Jeans (2006) did not discuss whether the fluctuations could be due to varying input of detrital kaolinite, but instead explored inconclusively the possibility that the fluctuations are caused by varying intensity of illitization of smectite. In the same review, Jeans (2006) also considered that there was a problematic lack of Al and Si for kaolinite formation in the now kaolinite-rich horizons of the Kimmeridge Clay formation, and because of this suggested that the source of these elements must have been volcanic, albeit from a poorly located source. However, inferences about the origins of the clay minerals from this stratigraphically limited sample set from the RGGE boreholes are not supported by petrographic data.

To investigate further the extent of diagenetic clay mineral formation within Kimmeridge Clay in Dorset, backscatter scanning electron microscopy (BSEM) was undertaken on selected subsamples of the suite already analysed by XRD. These nine subsamples were chosen to represent a range of high and low kaolinite/illite ratios from throughout the formation (Fig. 3). Of the samples analysed, only one near the top of the formation (46.79 m) showed evidence of significant diagenetic kaolinite, in this case by *in situ* replacement of pre-existing grains (Fig. 4a). Remnants of the grains are seldom detected, but the shape of the cavity and the morphology of the kaolinite suggest that feldspar rather than mica was the parent mineral. This sample corresponds to a clear peak in XRD-determined kaolinite/illite ratio. It should be noted that the kaolinite crystallites are *c*. 5 μm wide; that is, too big to be included in the clay fraction analysed by XRD unless broken up into single crystallites by the sample preparation method; we believe that this is what has happened.

This interval of occurrence of diagenetic kaolinite at the top of the Kimmeridge Clay Formation corresponds to an interval of only modest Th/K ratios from spectral gamma-ray data. Given the low solubility of thorium (e.g. Langmuir & Herman 1980) in the pore waters in which the kaolinite will have grown, this observation is unsurprising, and suggests that Th/K estimates based on spectral gamma-ray data used in conjunction with spot XRD analyses of clay mineralogy will pinpoint intervals of diagenetic kaolinite growth; specifically where low Th/K ratios correspond to high kaolinite/illite ratios.

One other examined level (344.27 m) showed evidence of minor replacement of mica by kaolinite (Fig. 5c). The other samples examined, and illustrated from 574.71 m (Fig. 5b) and 259.34 m (Fig. 5d), show no evidence of diagenetic kaolinite either in the matrix or as replacing grains. This observation is surprising for the sample from 574.71 m because despite high kaolinite/illite ratios this lower interval of the Kimmeridge Clay is also characterized by relatively low Th/K ratios. This anomaly may arise from the small-scale interbedding of silty and non-silty mudstones at the condensed base of the formation and consequent strong localization of the occurrence of diagenetic or detrital kaolinite. For this reason we have connected the lowermost five samples with a dashed line in Figure 3, and treat with suspicion the implied humid weathering conditions for the earliest Kimmeridgian.

Further observations were made using energy-dispersive X-ray analysis (EDS) of matrix in polished thin sections (carbon coated and examined in a JEOL6310 with Oxford Instruments INCA X-ray analytical software). In particular, the Al/K ratio was used as a proxy for kaolinite/illite ratio. This approach is valid because illite is the main K-bearing clay present in the Kimmeridge Clay assemblages. The results are shown in a cross plot of EDS-derived matrix Al/K ratio and XRD-derived kaolinite/illite ratio (Fig. 6). The sample at 46.79 m (21/2) clearly contains excess kaolinite over illite compared with all other analysed samples. The sample at 574.71 m (78/2) contains excess kaolinite for the

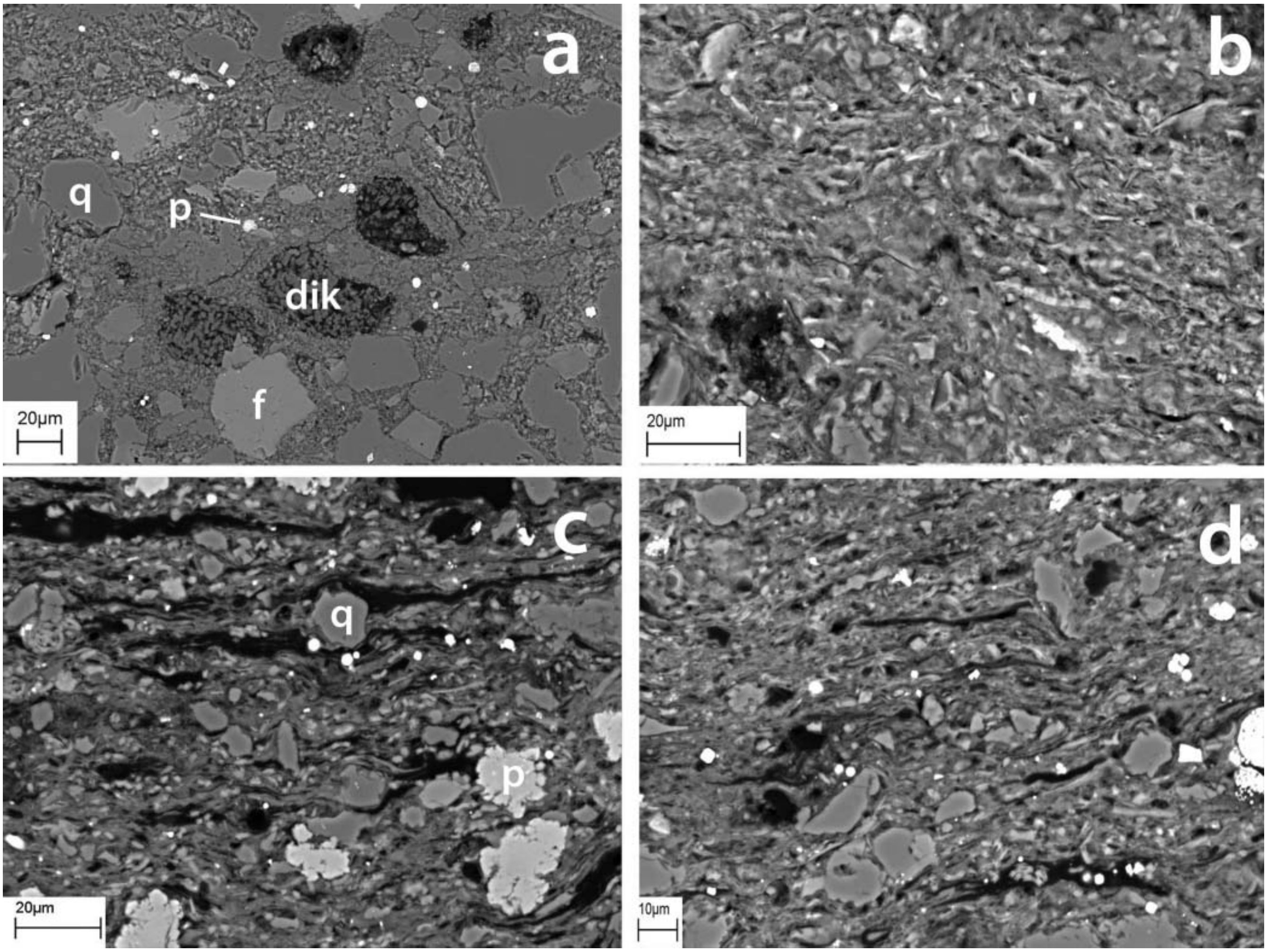

Fig. 5. BSEM images from selected core samples. Dark grey grains are quartz (q), pale grey is K feldspar (f), and white crystals are pyrite (p). (**a**) Void-filling diagenetic kaolinite (dik) within former feldspar silt grains (sample SQ1/21/2; 46.79 m). This sample demonstrates clear post-compactional kaolinite formation. (**b**) Homogeneous, unaltered detrital clay matrix (illitic clay and kaolinite) with silt and clay grade quartz grains (sample MH1/78/2; 574.71 m). (**c**) Detrital kaolinite-rich clasts present within clay matrix (sample SQ1/143/7; 344.27 m). (**d**) Unaltered mudstone matrix (sample SQ/109/10; 259.34 m). This sample is very similar in composition to MH1/78/2; 574.71 m.

measured Al/K ratio, but plots close to other measured samples. It might also be considered instructive to compare Al/K ratios against spectral gamma ray (SGR) derived Th/K ratios, as the latter should also increase with increasing kaolinite/illite ratio; however, the spatial scales represented by these elemental data are so different that meaningful comparisons are not possible (i.e. 10^{-4} v. 10^{1} cm).

Regional data comparisons and contrasts

Diagenetic changes

In the Kimmeridge Clay of the Cleveland Basin, Yorkshire, NE England (see Fig. 1 for locations), a similar composition of clay-mineral assemblages has been described by Herbin *et al.* (1991) from four boreholes (about 30% of illite, 40% of kaolinite and 30% I–S). These workers suggested that clay assemblages have undergone some burial diagenetic transformations, mainly from smectite to illite–smectite, whereas kaolinite is considered detrital. In contrast, Herbin *et al.* indicated that the total burial depth, estimated at a maximum of 1000–1400 m, is insufficient to have achieved complete transformation of smectite. Furthermore, the weakly mature organic matter, with an average T_{max} of 428 °C, would have been compatible with the occurrence of primary smectite. For example, in the Kimmeridgian–Tithonian deposits of the Boulonnais, northern France (Fig. 1), where smectite-rich intervals have been identified (Deconinck *et al.* 1983), the T_{max} values range between 413 and 434 °C (El Albani *et al.* 1993) with an average of 426 °C, very close to the average value recorded in the Cleveland Basin, and even higher than values from Dorset. Consequently, smectite probably never was deposited as detrital particles in the Kimmeridge Clay of either the Cleveland Basin or in the SW part of the Wessex Basins because its survival would have been compatible with the diagenetic state of organic matter.

Comparison of data between the Cleveland and Wessex basins is informative, although for the Cleveland Basin, only percentages of clay minerals are available, rather than the kaolinite/illite ratio, and these only for sediments from the *mutabilis* Zone upwards. In the Cleveland Basin, kaolinite-

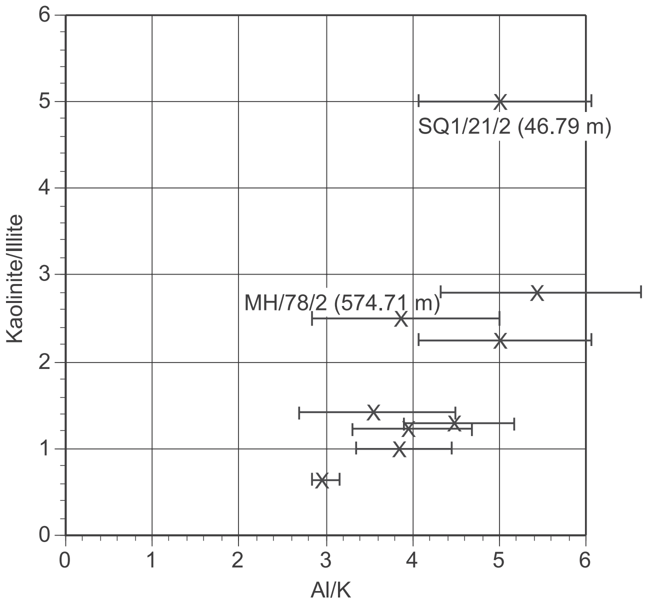

Fig. 6. Cross plot of Al/K (EDS) v. kaolinite/illite (XRD) for selected core samples. It should be noted that sample SQ1/21/2, 46.79 m, contains excess kaolinite over illite in comparison with Al/K values of other samples, and from BSEM images clearly contains diagenetic kaolinite (see Fig. 5a). Bars represent one standard deviation, where $n = 5-10$.

depleted intervals (<30% kaolinite) occur in the *mutabilis* Zone and from the *scitulus* Zone upward, whereas the *eudoxus*, *autissiodorensis* and *elegans* zones are kaolinite-rich (>30%). Thus, stratigraphic trends in the distribution of clay minerals in the Cleveland and Wessex Basins are similar, indicating that the detrital sources and the controlling factors of the clay sedimentation were the same in both cases. In addition, it is unlikely that the same diagenetic overprint occurs in two different sedimentary basins, strongly supporting, in agreement with Jeans (2006), the detrital origin of most clay minerals from the Kimmeridge Clay in both cases.

Detrital sources

In the northern Paris Basin, the Kimmeridgian–Tithonian sediments are exposed along coastal cliffs in Normandy and the Boulonnais. In the Boulonnais (Fig. 1) the outcrops have been intensively studied (Oschmann 1988, 1990; Geyssant *et al*. 1993; Proust *et al*. 1993, 1995; Herbin *et al*. 1995; Wignall & Newton 2001). The base of the Kimmeridgian is not exposed in the Boulonnais but it is in Normandy (Sansom *et al*. 1996). Therefore an almost complete composite sedimentary succession of the Kimmeridgian from the northern Paris Basin is available. The clay mineralogy of these deposits was first studied in the Boulonnais by Deconinck *et al*. (1983), and in Normandy by Saint-Germès *et al*. (1996). In comparison with the mineralogy of the Kimmeridge Clay of the UK, the French sections show major differences, but also some common features.

A particular difference is that in the Paris Basin sections smectite-rich strata occur in the Kimmeridgian upper *cymodoce* Zone and upper *orthocera* Subzone of the *mutabilis* Zone, and in the Tithonian *scitulus–wheatleyensis* zones and *rotunda–fittoni–albani* zones. In other neighbouring regions, such as the Jura Mountains (Colombié 2002), the Vocontian Trough (Deconinck 1992), Charentes (J.-F. Deconinck, unpubl. data), and the North Sea (Shaw & Primmer 1991), the clay mineralogy of Kimmeridgian sediments is similar to that of the Wessex and Cleveland basins, dominated by illite, kaolinite, and illite–smectite mixed layers. Thus, the occurrence of smectite in the northern Paris Basin is unusual, and seems to be controlled by local conditions. The landmass of the London–Brabant Massif was the likely source of detrital particles in the nearshore facies, at least in the Boulonnais. The low relief of this landmass would have been favourable to the steady-state erosion of smectite-rich soils. A similar pattern of clay minerals is recorded in the Oxfordian of the NE Paris Basin (Pellenard & Deconinck 2006) and smectite thus appears to constitute, during the Late Jurassic, a fingerprint of detritus from the London–Brabant Massif.

In discussion of sediment provenance into the Wessex Basin, Hallam & Sellwood (1976) have suggested that the London–Brabant Massif was also the likely source. The sources of detrital clays in the Kimmeridge Clay have been further discussed by Taylor *et al*. (2001), who concluded that clay minerals were probably derived from local landmasses, including Cornubia, and the Welsh, Irish, and London–Brabant massifs (Fig. 1). However, because of the absence of smectite-rich I–S clays in the Wessex and Cleveland basins, except in some samples from the *eudoxus* Zone, it is unlikely that the erosion of the London–Brabant massif would have contributed significantly to the supply of clays in the Kimmeridge Clay. This inference is compatible with the suggestion of Wignall (1994) that the London–Brabant Massif was submerged from deposition of the *eudoxus* Zone upward, except in the Boulonnais area where some depositional environments are extremely shallow or even probably emergent. In the Wealden Group of Early Cretaceous age in the Wessex and Weald basins, the detrital sources traced by heavy minerals suggest that most terrigenous influences were from the massifs of Cornubia and Armorica, whereas the contribution of the London–Brabant massif was negligible (Allen 1972).

Consideration of K/Ar signatures from two samples of the Kimmeridge Clay, and numerous samples from other Mesozoic mudrocks, suggested to Jeans *et al*. (2001) that the illite is originally of ‘Caledonian’ origin, and the kaolinite derived from unlocated Devonian and Carboniferous rocks. However, this latter mineral may equally well be derived from soils formed during the Late Jurassic, as is implied by our results.

The very large stratigraphic variations of clay assemblages in the NW Paris Basin (Fig. 7) in comparison with the Wessex and Cleveland Basins may be explained by deposition in varied sedimentary environments ranging from upper shoreface to lower offshore (Proust *et al*. 1995; Wignall & Newton 2001). Fluctuations of clay minerals have been tentatively explained by occasional tectonic rejuvenation of the London–Brabant massif (Deconinck *et al*. 1983). The influence of tectonic movements was formerly deduced from the sharp changes in clay mineralogy, but a biostratigraphic revision (Geyssant *et al*. 1993) now reveals that the sharpness results from stratigraphic condensation (e.g. between the Argiles de la Crèche and the Argiles de Wimereux, where two ammonite zones, *hudlestoni* and *pectinatus*, are missing (Fig. 7). The most striking feature of the Boulonnais succession is the unusual occurrence of smectite in the shallowest environments, when usually this mineral is preferentially deposited in quiet offshore settings. A similar trend is observed in the underlying Oxfordian sediments (Schnyder *et al*. 2000). This can be explained by the fact that during sea-level lowstand, the London–Brabant massif was emerged and might provide detrital smectite. In contrast, during sea-level highstand, the London–Brabant massif was probably submerged and clay sedimentation was dominated by illite, kaolinite and I–S mixed-layer clays originating from more distant massifs.

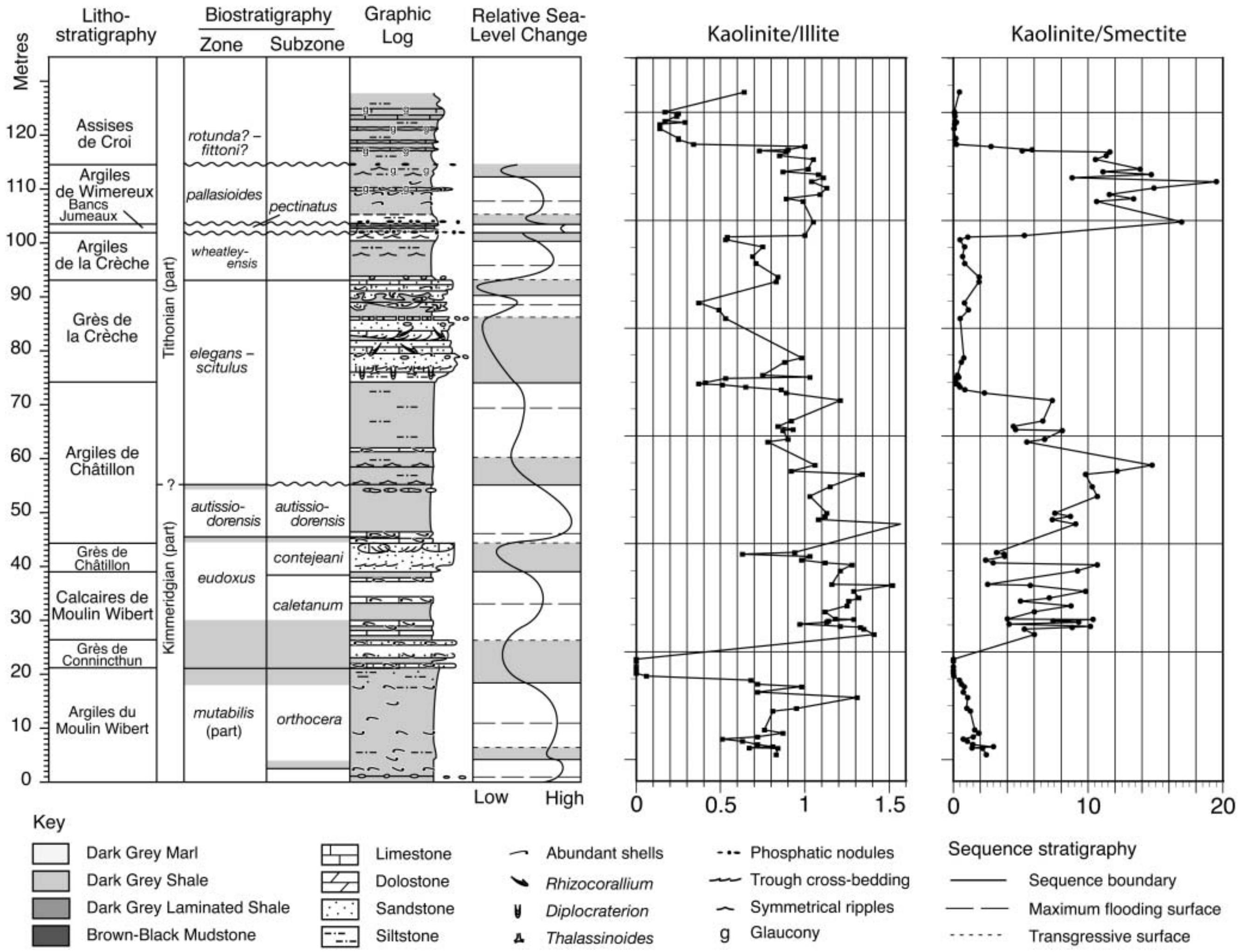

Fig. 7. Clay mineralogy of the Boulonnais section with summary lithological log. Lithological log modified from Williams *et al*. (2001). Clay mineral data from Deconinck *et al*. (1983).

Palaeoclimatic influences

The common features between the Wessex and the NW Paris basins concern the relative proportions of kaolinite. The kaolinite-depleted intervals are coeval in the Paris Basin and in the Wessex and Cleveland Basins. Two kaolinite-depleted intervals occur consistently; in the *cymodoce* Zone to the *orthocera* Subzone, and in the *wheatleyensis* and *hudlestoni* zones. This suggests two corresponding arid phases, the second being that previously identified from facies and mineralogical composition of the sediments (Wignall & Ruffell 1990). In the Boulonnais, the sediments from the *mutabilis* Zone contain a significant proportion of the pollen *Classopolis*, consistent with arid conditions (Schnyder 2003). Another feature common to both regions is the abundance of kaolinite in the *eudoxus*, *autissiodorensis* and *elegans* zones, and to a lesser extent in the *pallasioides* Zone, indicating more humid conditions. Looking at the evolution of the kaolinite/smectite ratio from the Boulonnais section (Fig. 7), the alternation of arid and humid phases is particularly clear, albeit enhanced by hiatuses.

The differences in clay mineralogy of proximal (northern Paris Basin) and distal environments (Wessex and Cleveland basins) result mainly from the local environmental conditions, but the common features seem to be controlled by regional fluctuations from arid to humid climates.

Looking further afield, clay mineral data from the Kimmeridgian and Volgian of the Russian platform show the same trend, although there are difficulties of correlation of the sections with those of the Wessex, Cleveland and Paris basins because of different ammonite assemblages. Figure 8 shows some of the salient features from these locations. Like the clay assemblages of the Wessex and Cleveland basins, those of the Russian platform are composed of illite, illite–smectite mixed layers, and kaolinite (Schnyder 2003). In the *baylei* and *cymodoce* zones, percentages of kaolinite are quoted as $<20\%$, whereas in the *eudoxus* and *autissiodorensis* zones they estimated as 20–40% (the *mutabilis* Zone is missing). The first arid phase recorded in NW Europe in the *cymodoce* and *mutabilis* zones, and the transition to more humid climate in the *eudoxus* and *autissiodorensis* zones, is particularly well recorded also on the Russian platform.

Unfortunately, the *pseudoscythica* Zone that should correspond to the *hudlestoni* and *pectinatus* arid phase evidenced in NW Europe is highly condensed on the Russian platform, and therefore even if the arid phase had occurred there, it is not recorded. Upwards, the base of the *panderi* Zone, which may correspond

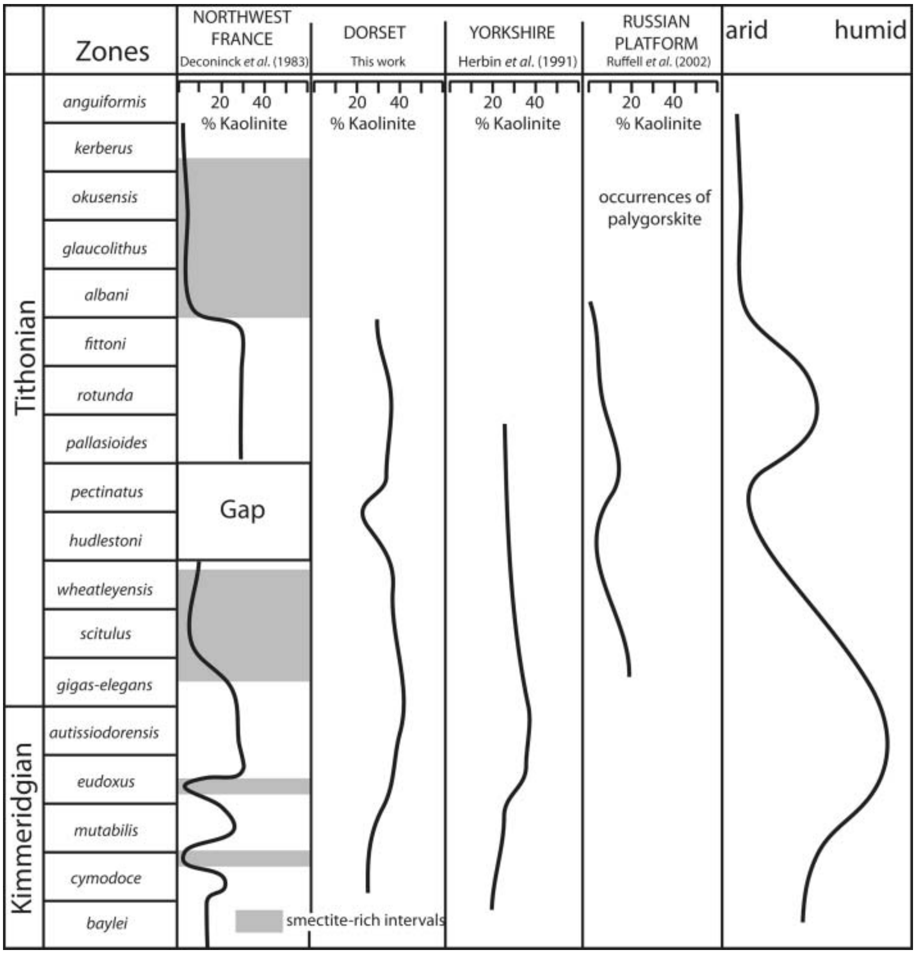

Fig. 8. Summary of main trends in clay mineral content through the Kimmeridgian–Tithonian interval and implied palaeoclimatic change.

to the *pallasioides* Zone, has kaolinite in abundance, indicating humid conditions akin to those of the Boulonnais and England. In the upper part of the *panderi*, *virgatites* and *nikitini* ammonite zones corresponding to the latest Tithonian, kaolinite is much less abundant and occasional occurrences of palygorskite are recorded, which may correspond to the arid phase inferred for western Europe at the Jurassic–Cretaceous boundary (Ruffell *et al*. 2002; Riboulleau *et al*. 2003; Schnyder 2003). The climatic evolution recorded in the Kimmeridgian of France and England is likely to extend to a much wider area.

The arid phase starting in the early Tithonian ends in the early Berriasian, where the proportions of kaolinite increase sharply in several sedimentary basins located either in the boreal realm or on the northern and southern margins of the Tethys (Deconinck 1993; Schnyder *et al*. 2005). The return to more humid conditions is apparently synchronous. The review presented by Price (1999) shows evidence of glacial conditions from sediments deposited at high palaeolatitudes around the Jurassic–Cretaceous boundary. A relatively short-lived ice-house mode is therefore suggested on the basis of sedimentary deposits. This cooler interval through the Tithonian is consistent with the development of aridity mainly recorded by a severe depletion of kaolinite and palynological data. The rapidity, reversibility, and regionally synchronous changes in palaeoclimate outlined on the basis of the clay mineral data rule out large-scale tectonic factors such as mountain building or continental rotations as the cause of climate change. The extent to which cyclic changes at the decametric scale correspond to 100 kyr or 400 kyr Milankovitch cycles (see Weedon *et al*. 2004) remains to be further investigated.

Conclusions

Clay mineral assemblages through the Kimmeridge Clay Formation close to the type section at Kimmeridge, Dorset, comprise predominantly illite and kaolinite, with subsidiary quantities of random illite–smectite mixed layers. The occurrence of authigenic kaolinite is only locally important and can be recognized on the basis of SEM observations and degree of crystallinity from examination of XRD traces.

Detrital kaolinite/illite ratios change progressively and cyclically through the Kimmeridgian and Tithonian. Changes in kaolinite/illite ratio are mirrored at a large scale (*c*. 100 m) and at a small scale (*c*. 10 m) by Th/K ratios recorded in the spectral gamma-ray log. Authigenic kaolinite has no impact on Th/K ratios, allowing the spectral gamma-ray log to be used in conjunction with XRD analysis as a qualitative index of kaolinite authigenesis (XRD indication of high kaolinite/illite ratio combined with low Th/K ratio).

The clay mineral trends are similar in the Cleveland and Wessex basins, suggesting common detrital sources. Clay mineralogy through Late Jurassic successions of southern England and northern France and Russia indicates consistently alternating humid and arid phases. Kaolinite-depleted intervals characterized arid climatic conditions represented by the *cymodoce–mutabilis* zones and the *hudlestoni*–lower *pectinatus* zones. By contrast *eudoxus–autissiodorensis* zones and the *pallasioides* Zone seem to have been relatively humid, with a return to aridity in the *rotunda–fittoni* zones. Superimposed on these long time-scale trends are short time-scale (Milankovitch) fluctuations, some of them very large, which probably also reflect the effects of palaeoclimatic cycles.

The abrupt climate change toward more arid environments previously identified as occurring in the *hudlestoni* Zone is supported by the expanded dataset of the present paper. However, rather than representing a step-change in long-term palaeoclimatic change, the newly presented data instead indicate that the *hudlestoni* Zone represents a transient mid-Tithonian culmination of a trend towards aridity that began in the earliest Tithonian, was subsequently reversed, and then resumed in the latest Tithonian. This aridity, ending in the Berriasian, coincides with the cold interval and ice-house conditions recorded around the Jurassic–Cretaceous boundary, and suggests a relationship between cold and arid conditions during the latest Jurassic and the earliest Cretaceous.

The RGGE project was funded by NERC (GST/02/1346 and GST/06/1346) and the following companies, here listed under their original names (*c*. 1997): ARCO British, Conoco Norway, Enterprise Oil, FINA Exploration, Phillips Petroleum, Saga Petroleum, Shell UK Exploration and Production, Statoil (UK), and Texaco. We thank P. Wignall and an anonymous referee for their insightful comments.

References

Abbink, O., Targarona, J., Brinkhuis, H. & Visscher, H. 2001. Late Jurassic to earliest Cretaceous palaeoclimatic evolution of the southern North Sea. *Global and Planetary Change*, **30**, 231–256.

Allen, P. 1972. Wealden detrital tourmaline: implications for north-western Europe. *Journal of the Geological Society, London*, **128**, 273–294.

Brereton, N.R., Gallois, R.W. & Whittaker, A. 2001. Enhanced lithological description of a Jurassic mudrock sequence using geophysical wireline logs. *Petroleum Geoscience*, **7**, 315–320.

Brown, G. & Brindley, G.W. 1980. X-ray diffraction procedures for clay mineral identification. *In:* Brindley, G.W. & Brown, G. (eds) *Crystal Structures of Clay Minerals and their X-ray Identification*. Mineralogical Society, London, Monograph, **5**, 305–360.

Burley, S.D. & Macquaker, J.H.S. 1992. Authigenic clays, diagenetic sequences and conceptual diagenetic models in contrasting basin-margin and basin-center North Sea Jurassic sandstones and mudstones. *In:* Houseknecht, D.W. & Pittman, E.D. (eds) *Origin, Diagenesis and Petrophysics of Clay Minerals in Sandstones*. SEPM Special Publications, **47**, 81–110.

Butler, M. 1998. The geological history of the southern Wessex Basin—a review of new information from oil exploration. *In:* Underhill, J.R. (ed.) *Development, Evolution and Petroleum Geology of the Wessex Basin*. Geological Society, London, Special Publications, **133**, 67–86.

Caron, M., Robaszynski, F., Amédro, F., *et al.* 1999. Estimation de la durée de l'événement anoxique global au passage Cénomanien/Turonien. Approche cyclostratigraphique dans la formation Bahloul en Tunisie centrale. *Bulletin de la Societé Géologique de France*, **170**, 145–160.

Chadwick, R.A. 1985. Upper Jurassic to Cretaceous sedimentation and subsidence. *In:* Whittaker, A. (ed.) *Atlas of Onshore Sedimentary Basins in England and Wales: Post-Carboniferous Tectonics and Stratigraphy*. Blackie, Glasgow.

Chambers, M.H. 2006. *A high-resolution mineralogical study and chemostratigraphy of the UK onshore Kimmeridge Clay Formation*. PhD thesis, University of Reading.

Colombié, C. 2002. *Sédimentologie, stratigraphie séquentielle et cyclostratigraphie du Kimméridgien du Jura suisse et du bassin vocontien (France): Relations plate-forme–bassin et facteurs déterminants*. Geofocus, **4**.

Cope, J.C.W., Duff, K.L., Parsons, C.F., Torrens, H.S., Wimbledon, W.A. & Wright, J.K. 1980. *A correlation of Jurassic rocks in the British Isles. Part Two: Middle and Upper Jurassic*. Geological Society, London, Special Reports, **15**.

Deconinck, J.-F. 1987. Minéraux argileux des faciès purbeckiens: Jura suisse et français, Dorset (Angleterre) et Boulonnais (France). *Annales de la Société Géologique du Nord*, **CVI**, 285–297.

Deconinck, J.-F. 1992. *Sédimentologie des argiles dans le Jurassique–Crétacé d'Europe occidentale et du Maroc*. Mémoir Habilitation, Université Lille 1.

Deconinck, J.-F. 1993. Clay mineralogy of the Late Tithonian–Berriasian deep-sea carbonates of the Vocontian Trough (SE France): relationships with sequence stratigraphy. *Bulletin des Centres de Recherche Exploration–Production Elf Aquitaine*, **17**, 223–234.

Deconinck, J.-F., Chamley, H., Debrabant, P. & Colbeaux, J.P. 1983. Le Boulonnais au Jurassique supérieur: données de la minéralogie des argiles et de la géochimie. *Annales de la Société Géologique du Nord*, **102**, 145–152.

Deconinck, J.-F., Hesselbo, S.P., Debuisser, N., Averbuch, O., Baudin, F. & Bessa, J. 2003. Environmental controls on clay mineralogy of an Early Jurassic mudrock (Blue Lias Formation, southern England). *International Journal of Earth Sciences*, **92**, 255–266.

El Albani, A., Deconinck, J.-F., Herbin, J.P. & Proust, J.N. 1993. Caractérisation géochimique de la matière organique et minéralogie des argiles du Kimméridgien du Boulonnais. *Annales de la Société Géologique du Nord, 2ème série*, **2**, 113–120.

Gallois, R. 1973. Some detailed correlations in the Upper Kimmeridge Clay in Norfolk and Lincolnshire. *Bulletin of the Geological Survey of Great Britain*, **44**, 63–75.

Gallois, R. 2000. The stratigraphy of the Kimmeridge Clay Formation (Upper Jurassic) in the RGGE Project boreholes at Swanworth Quarry and Metherhills, south Dorset. *Proceedings of the Geologists' Association*, **111**, 265–280.

Geyssant, J.R., Vidier, J.P., Herbin, J.P., Proust, J.N. & Deconinck, J.-F. 1993. Biostratigraphie et paléoenvironnement des couches de passage Kimméridgien/Tithonien du Boulonnais (Pas de Calais): nouvelles données paléontologiques (ammonites) organisation séquentielle et contenu en matière organique. *Géologie de la France*, **4**, 11–24.

Gradstein, F.M., Ogg, J.G., Smith, A.G., Bleeker, W. & Lourens, L.J. 2004. A new Geologic Time Scale, with special reference to the Precambrian and Neogene. *Episodes*, **27**, 83–100.

Hallam, A. 1984. Continental humid and arid zones during the Jurassic and Cretaceous. *Palaeogeography, Palaeoclimatology, Palaeoecology*, **47**, 195–223.

Hallam, A. 1993. Jurassic climates as inferred from the sedimentary and fossil record. *Philosophical Transactions of the Royal Society of London, Series B*, **341**, 287–296.

Hallam, A. & Sellwood, B.W. 1976. Middle Mesozoic sedimentation in relation to tectonics in the British area. *Journal of Geology*, **84**, 301–321.

Hallam, A., Grose, J.A. & Ruffell, A.H. 1991. Palaeoclimatic significance of changes in clay mineralogy across the Jurassic–Cretaceous boundary in England and France. *Palaeogeography, Palaeoclimatology, Palaeoecology*, **81**, 173–187.

Hassan, M.H.A. & Hossin, A. 1975. Contribution à l'étude des comportements du thorium et du potassium dans les roches sédimentaires. *Comptes Rendus de l'Académie des Sciences, Série D: Sciences Naturelles*, **280**, 533–535.

Herbin, J.P., Müller, C., Geyssant, J.R., Mélières, F., Penn, I.E. & le groupe Yorkim 1991. Hétérogénéité quantitative et qualitative de la matière organique dans les argiles du Val de Pickering (Yorkshire, UK). Cadre sédimentologique et stratigraphique. *Revue de l'Institut Français du Pétrole*, **46**, 675–712.

Herbin J.P., Geyssant J.R., *et al.* 1995. Sequence stratigraphy of source rocks applied to the study of the Kimmeridgian/Tithonian in the north-west European shelf (Dorset/UK, Yorkshire/UK and Boulonnais/France). *Marine and Petroleum Geology*, **12**, 177–194.

Hesselbo, S.P. 1996. Spectral gamma-ray logs in relation to clay mineralogy and sequence stratigraphy, Cenozoic of the Atlantic margin, offshore New Jersey. *In:* Mountain, G.S., Miller, K.G., Blum, P., Poag, C.W. & Twitchell, D.C. (eds) *Proceedings of the Ocean Drilling Program; Scientific Results, 150*. Ocean Drilling Program, College Station, TX, 411–422.

Holtzapffel, T. 1985. *Les Minéraux Argileux. Préparation, Analyse Diffractométrique et Détermination*. Société Géologique du Nord, Publication, **12**.

Jeans, C.V. 2006. Clay mineralogy of the Jurassic strata of the British Isles. *Clay Minerals*, **41**, 187–307.

Jeans, C.V., Mitchell, J.G., Fischer, M.J., Wray, D.S. & Hall, I.R. 2001. Age, origin and climatic signal of English Mesozoic clays based on K/Ar signatures. *Clay Minerals*, **36**, 515–539.

Lallier-Vergès, E., Bertrand, P., Huc, A.Y., Bückel, D. & Tremblay, P. 1993. Control of the preservation of organic matter by productivity and sulphate reduction in Kimmeridgian shales from Dorset (UK). *Marine and Petroleum Geology*, **10**, 600–605.

Langmuir, D. & Herman, J.S. 1980. The mobility of thorium in natural waters at low temperatures. *Geochimica et Cosmochimica Acta*, **44**, 1753–1766.

Macquaker, J.H.S. & Gawthorpe, R.L. 1993. Mudstone lithofacies in the Kimmeridge Clay Formation, Wessex Basin, Southern England: implications for the origin and controls of the distribution of mudstones. *Journal of Sedimentary Petrology*, **63**, 1129–1143.

MELNYK, D.H., ATHERSUCH, J. & SMITH, D.G. 1992. Estimating the dispersion of biostratigraphic events in the subsurface by graphic correlation—an example from the Late Jurassic of the Wessex Basin, UK. *Marine and Petroleum Geology*, **9**, 602–607.

MELNYK, D.H., SMITH, D.G. & AMIRI-GARROUSSI, K. 1994. Filtering and frequency mapping as tools in subsurface cyclostratigraphy, with examples from the Wessex Basin, UK. *In:* DE BOER, P.L. & SMITH, D.G. (eds) *Orbital Forcing and Cyclic Sequences*. Blackwell Scientific, Oxford, 35–46.

MOORE, D.M. & REYNOLDS, R.C., JR 1997. *X-Ray Diffraction and the Identification and Analysis of Clay Minerals*, 2nd edn. Oxford University Press, Oxford.

MORGANS-BELL, H.S., COE, A.L., HESSELBO, S.P., ET AL. 2001. Integrated stratigraphy of the Kimmeridge Clay Formation (Upper Jurassic) based on exposures and boreholes in south Dorset, UK. *Geological Magazine*, **138**, 511–539.

MYERS, K.J. & WIGNALL, P.B. 1987. Understanding Jurassic organic-rich mudrocks—New concepts using gamma-ray spectrometry and palaeoecology: examples from the Kimmeridge Clay of Dorset and the Jet Rock of Yorkshire. *In:* LEGGETT, J. K. & ZUFFA, G. G. (eds) *Marine Clastic Sedimentology.* Graham and Trotman, London, 172–189.

OGG, J.G., HASENYAGER, R.W., II & WIMBLEDON, W.A. 1994. Jurassic–Cretaceous boundary: Portland–Purbeck magnetostratigraphy and possible correlation to the Tethyan faunal realm. *Geobios, M.S.*, **17**, 519–527.

OSCHMANN, W. 1988. Kimmeridge Clay sedimentation—a new cyclic model. *Palaeogeography, Palaeoclimatology, Palaeoecology*, **65**, 217–251.

OSCHMANN, W. 1990. Environmental cycles in the Late Jurassic northwest European epeiric basin: interaction with atmospheric and hydrospheric circulations. *Sedimentary Geology*, **69**, 313–332.

PELLENARD, P. & DECONINCK, J.-F. 2006. Mineralogical variability of Callovo-Oxfordian clays from the Paris Basin and the Subalpine Basin. *Comptes Rendus Géosciences*, **338**, 854–866.

PENN, I.E., COX, B.M. & GALLOIS, R.W. 1986. Towards precision in stratigraphy–geophysical log correlation of Upper Jurassic (including Callovian) strata of the Eastern England Shelf. *Journal of the Geological Society, London*, **143**, 381–410.

PRICE, G. 1999. The evidence and implications of polar ice during the Mesozoic. *Earth-Science Reviews*, **48**, 183-210.

PROUST, J.N., DECONINCK, J.-F., GEYSSANT, J.R., HERBIN, J.P. & VIDIER, J.P. 1993. Nouvelles données sédimentologiques dans le Kimméridgien et le Tithonien du Boulonnais. *Comptes Rendus de l'Académie des Sciences*, **316**, 363–369.

PROUST, J.N., DECONINCK, J.F., GEYSSANT, J.R., HERBIN, J.P. & VIDIER, J.P. 1995. Sequence analytical approach to the Upper Kimmeridgian–Lower Tithonian storm-dominated ramp deposits of the Boulonnais (Northern France). A landward time-equivalent to offshore marine source rocks. *Geologische Rundschau*, **84**, 255–271.

QUIREIN, J.A., GARDNER, J.S. & WATSON, J.T. 1982. Combined natural gamma ray spectral/litho-density measurements applied to complex lithologies. SPE 11143, 57th Annual Fall Technical Conference and Exhibition of the Society of Petroleum Engineers of AIME, New Orleans, LA.

REES, P.MC.A., ZIEGLER, A.M. & VALDES, P.J. 2000. Jurassic phytogeography and climates: new data and modern comparisons. *In:* HUBER, B.T., MACLEOD, K.G. & WING, S.L. (eds) *Warm Climates in Earth History.* Cambridge University Press, Cambridge, 297–318.

RIBOULLEAU, A., BAUDIN, F., DECONINCK, J.F., DERENNE, S., LARGEAU, C. & TRIBOVILLARD, N. 2003. Depositional conditions and organic matter preservation pathways in an epicontinental environment: the Upper Jurassic Kashpir Oil Shales (Volga Basin, Russia). *Palaeogeography, Palaeoclimatology, Palaeoecology*, **197**, 171–197.

RIDER, M.H. 1996. *Geological Interpretation of Well Logs*, 2nd edn. Whittles, Caithness.

RUFFELL, A.H. & WORDEN, R. 2000. Palaeoclimate analysis using spectral gamma-ray data from the Aptian (Cretaceous) of southern England and southern France. *Palaeogeography, Palaeoclimatology, Palaeoecology*, **155**, 265–283.

RUFFELL, A.H., PRICE, G.D., MUTTERLOSE, J., KESSELS, K., BARABOSHKIN, E. & GRÖCKE, D.R. 2002. Palaeoclimate indicators (clay minerals, calcareous nannofossils, stable isotopes) compared from two successions in the late Jurassic of the Volga Basin (SE Russia). *Geological Journal*, **37**, 17–33.

SAINT-GERMÈS, M., BAUDIN, F., DECONINCK, J.F., HANTZPERGUE, P. & SAMSON, Y. 1996. Sédimentologie de la matière organique et des argiles du Kimméridgien de Normandie (Région du Havre). *Géologie de la France*, **3**, 21–33.

SANSOM, Y., LEPAGE, G., HANTZPERGUE, P., GUYADER, J., SAINT-GERMÈS, M., BAUDIN, F. & BIGNOT, G. 1996. Révision lithostratigraphique et biostratigraphique du Kimméridgien de la région havraise (Normandie). *Géologie de la France*, **3**, 3–19.

SCHNYDER, J. 2003. *Le passage Jurassique/Crétacé: événements instantanés, variations climatiques enregistrées dans les faciès purbeckiens français (Boulonnais, Charentes) et anglais (Dorset). Comparaison avec le domaine téthysien*. PhD thesis, Université Lille 1.

SCHNYDER, J., BAUDIN, F., DECONINCK, J.F., DURLET, C., JAN DU CHÊNE, R. & LATHUILIÈRE, B. 2000. Stratigraphie et analyse sédimentologique du passage Oxfordien/Kimméridgien dans le Boulonnais. *Géologie de la France*, **4**, 21–37.

SCHNYDER, J., GORIN, G., BAUDIN, F., DECONINCK, J.F. & SOUSSI, M. 2005. Enregistrement de la variation climatique du passage Jurassique/Crétacé sur la marge sud de la Téthys: minéralogie des argiles et palynofaciès de la coupe du Jebel Meloussi en Tunisie (Formation Sidi Kralif). *Bulletin de la Societé Géologique de France*, **176**, 171–182.

SCHNYDER, J., RUFFELL, A.H., DECONINCK, J.F. & BAUDIN, F. 2006. Conjunctive use of spectral gamma-ray logs and clay mineralogy in defining late Jurassic–early Cretaceous palaeoclimate change (Dorset, U.K.). *Palaeogeography, Palaeoclimatology, Palaeoecology*, **229**, 303–320.

SCOTCHMAN, I.C. 1987*a*. Relationship between clay diagenesis and organic maturation in the Kimmeridge Clay Formation, onshore UK. *In:* BROOKS, J. & GLENNIE, K. (eds) *Petroleum Geology of North West Europe*. Graham & Trotman, London, 251–261.

SCOTCHMAN, I.C. 1987*b*. Clay diagenesis in the Kimmeridge Clay Formation, onshore UK, and its relation to organic maturation. *Mineralogical Magazine*, **51**, 535–551.

SCOTCHMAN, I.C. 1989. Diagenesis of the Kimmeridge Clay Formation, onshore UK. *Journal of the Geological Society, London*, **146**, 285–303.

SERRA, O., BALDWIN, J. & QUIREIN, J.A. 1980. Theory, interpretation and application of natural gamma ray spectroscopy. SPWLA 21st Annual Logging Symposium, Houston, Paper Q Appendix A, B.

SHAW, H.F. & PRIMMER, T.J. 1991. Diagenesis of mudrocks from the Kimmeridge Clay formation of the Brae Area, UK North Sea. *Marine and Petroleum Geology*, **8**, 270–277.

TAYLOR, S.P., SELLWOOD, B.W., GALLOIS, R.W. & CHAMBERS, M.H. 2001. A sequence stratigraphy of the Kimmeridgian and Bolonian stages (late Jurassic): Wessex–Weald Basin, southern England. *Journal of the Geological Society, London*, **158**, 179–192.

THIRY, M. 2000. Palaeoclimatic interpretation of clay minerals in marine deposits: an outlook from the continental origin. *Earth-Science Reviews*, **49**, 201–221, doi:10.1016/S0012-8252(99)00054-9.

WEEDON, G.P., JENKYNS, H.C., COE, A.L. & HESSELBO, S.P. 1999. Astronomical calibration of the Jurassic time-scale from cyclostratigraphy in British mudrock formations. *Philosophical Transactions of the Royal Society of London, Series A*, **357**, 1787–1813.

WEEDON, G.P., COE, A.L. & GALLOIS, R.W. 2004. Cyclostratigraphy, orbital tuning and inferred productivity for the type Kimmeridge Clay (Late Jurassic), Southern England. *Journal of the Geological Society, London*, **161**, 655–666.

WHITTAKER, A., HOLLIDAY, D.W. & PENN, I.E. 1985. *Geophysical Logs in British Stratigraphy.* Geological Society, London, Special Reports, **18**.

WIGNALL, P.B. 1994. *Black Shales*. Geology and Geophysics Monographs, **30**.

WIGNALL, P.B. & MYERS, K.J. 1988. Interpreting benthic oxygen levels in mudrocks: a new approach. *Geology*, **16**, 452–455.

WIGNALL, P.B. & NEWTON, R. 2001. Black shales on the basin margin: a model based on examples from the upper Jurassic of the Boulonnais, northern France. *Sedimentary Geology*, **144**, 335–356.

WIGNALL, P.B. & PICKERING, K.T. 1993. Paleoecology and sedimentology across a Jurassic fault scarp, NE Scotland. *Journal of the Geological Society, London*, **150**, 323–340.

WIGNALL, P.B. & RUFFELL, A.H. 1990. The influence of a sudden climatic change on marine deposition in the Kimmeridgian of northwest Europe. *Journal of the Geological Society, London*, **147**, 365–371.

WILLIAMS, C.J., HESSELBO, S.P., JENKYNS, H.C. & MORGANS-BELL, H.S. 2001. Quartz silt in mudrocks as a key to sequence stratigraphy (Kimmeridge Clay Formation, Late Jurassic, Wessex Basin, UK). *Terra Nova*, **13**, 449–455.

ZIEGLER, A.M., ESHEL, G., REES, P.MCA., ROTHFUS, T.A., ROWLEY, D.B. & SUNDERLIN, D. 2003. Tracing the tropics across land and sea: Permian to present. *Lethaia*, **36**, 227–254.

ZIEGLER, P.A. 1990. *Geological Atlas of Western and Central Europe*. Shell Internationale Petroleum Maatschappij B.V., The Hague.

Received 8 May 2009; revised typescript accepted 15 July 2009.
Scientific editing by John Marshall.